1-1-2014

Rapid profiling of laser-induced photochemistry in single microdroplets using mass spectrometry

Phillip J. Tracey
University of Wollongong, pjt105@uowmail.edu.au

Bartholomew S. Vaughn
University of Wollongong, bv703@uowmail.edu.au

Brendon J. Roberts
University of Wollongong, bjr955@uowmail.edu.au

Berwyck L. J Poad
University of Wollongong, bpoad@uow.edu.au

Adam J. Trevitt
University of Wollongong, adamt@uow.edu.au

Rapid profiling of laser-induced photochemistry in single microdroplets using mass spectrometry

Abstract

Rapid assessment of laser-induced photochemistry in single microdroplets is afforded by on-demand microdroplet generation coupled to a commercial ion-trap mass spectrometer. Single microdroplets (diameter 50 μm, 65 pL) fall on a steel needle held at +2 kV where they subsequently form a spray that is directed toward the inlet of an ion-trap mass spectrometer. It is demonstrated that single microdroplet mass spectra are recordable, one at a time, for methanol droplets containing 100 μM 4-iodoaniline. Extending on this, to probe laser-initiated photochemistry in single picoliter volumes, a UV laser pulse is timed to intercept the droplet before hitting the needle. Comparison of laser-on and laser-off mass spectra reveals the laser-initiated photochemical products. We demonstrate the technique by following UV laser initiated chemistry in methanol droplets containing 4-iodoaniline and 3-(iodomethyl)-N,N,N-trimethylbenzenamine and reveal numerous products within a few hundred single droplet experiments over several minutes. This technique allows for rapid detection of laser-initiated photochemistry in single picoliter volumes.

Keywords

GeoQuest

Publication Details

Tracey, P. J., Vaughn, B. S., Roberts, B. J., Poad, B. L. J. & Trevitt, A. J. (2014). Rapid profiling of laser-induced photochemistry in single microdroplets using mass spectrometry. Analytical Chemistry, 86 (6), 2895-2899.

Rapid profiling of laser-induced photochemistry in single microdroplets using mass spectrometry

Phillip J. Tracey, Bartholomew S. Vaughn, Brendon J. Roberts,

Berwyck L.J. Poad, Adam J. Trevitt*

School of Chemistry, University of Wollongong, New South Wales, 2522, Australia

***corresponding author: adamt@uow.edu.au**

Abstract

Rapid assessment of laser-induced photochemistry in single microdroplets is afforded by on-demand microdroplet generation coupled to a commercial ion-trap mass spectrometer. Single microdroplets (diameter ~50 μm, 65 pL) fall on a steel needle held at 2 kV where they subsequently form a spray that is directed towards the inlet of an ion-trap mass spectrometer. It is demonstrated that single microdroplet mass spectra are recordable, one at a time, for methanol droplets containing 100 μM 4-iodoaniline. Extending on this, to probe laser-initiated photochemistry in single picolitre volumes, a UV laser pulse is timed to intercept the droplet before hitting the needle. Comparison of laser-on and laser-off mass spectra reveals the laser-initiated photochemical products. We demonstrate the technique by following UV laser initiated chemistry in methanol droplets containing 4-iodoaniline and 3-(iodomethyl)-*N*,*N*,*N*-trimethylbenzenamine and reveal numerous products within a few hundred single droplet experiments over several minutes. This technique allows for rapid detection of laser-initiated photochemistry in single picolitre volumes.

Introduction

Photoactivated chemistry in liquid domains underpins many important atmospheric and biological processes. Photochemistry of atmospheric aerosols can have a profound effect on particle composition and growth, and these processes ultimately influence air quality and radiation forcing.[1] Recent studies have shown the importance of both direct photolysis in droplets[2] and heterogeneous particle photochemistry.[3] In biological contexts, light-induced DNA damage attributed to pyrimidine dimerization of adjacent nucleobases can result in mutagenic DNA.[4-6] Human developed phototherapies, on the other hand, are formulated to treat various diseases[7, 8] – a well-known example is the treatment of neonatal jaundice. Early studies showed the importance of photon wavelength on the efficacy of treatment.[9, 10] More recently, photodynamic therapies (PDTs) have been developed that rely on photoactivating molecules to bound, long-lifetime triplet states to regioselectively generate singlet O_2 molecules which then in turn attack nearby cancerous tissue.[11-13] The collision-mediated formation of singlet O_2 returns the sensitiser molecule to the ground electronic state where it is available again for photoexcitation. In such applications, high absorption cross sections are preferred but photodissociation is undesirable as it interrupts the PDT cycle, thwarting performance and can lead to undesirable chemical reactions.

In all of the above applications, an understanding of the photodissociation propensities and characterization of the photoproducts are vital details in understanding the chemistry in these diverse environments. Undertaking characterization studies in small volumes, with rapid and sensitive detection, is attractive particularly when complex chemistry is initiated and sample quantities are scant. Coupling liquid microdroplets to mass spectrometric detection can address these requirements.

Mass spectrometric studies of liquid droplets have been reported in the past, examples include the field induced droplet ionisation mass spectrometry (FIDI-MS) technique,[14, 15]

charge/matrix-assisted laser desorption/ionisation of acoustically levitated droplets,[16, 17] and droplet electrospray mass spectrometry (DES-MS).[18, 19] A number of these aerosol and single droplet mass spectrometric techniques have been recently reviewed by Laskin *et al.*[20] FIDI–MS experiments direct a microdroplet stream, created by a kHz rate vibrating orifice aerosol generator (VOAG), through pair of parallel plates that are pulsed with a high potential. The charged-spray emission is directed into the inlet of a mass spectrometer. More recently, the same desorption technique has been applied to a dangling liquid pendent to afford longer time scale experiments. This technique was used to probe ozonolysis at the surface of a liquid pendant of a solution containing a mixture of saturated and unsaturated lipids.[21]

In a similar experiment, DES-MS, a kHz vibrating orifice aerosol generator (VOAG) produced a droplet stream that free falls past a needle held at a high potential, charging the droplet stream resulting in a spray erupting from the surface of the droplets that was directed into a mass spectrometer for analysis.[19] The technique was demonstrated to desorb, ionise and detect a number of reference compounds from these droplets, including NaCl salts, 1,12-dodecyldiamine, potassium crown ether complexes, and tetraalkylamines.

For sensitive liquid photochemical analysis, complexities can arise when irradiating a stagnant sample as first generation photoproducts can in turn further dissociate with subsequent photon absorption, quickly complicating the analysis. Interactions with container walls can also perturb the chemistry. In this study, we demonstrate a new technique that couples on-demand single microdroplet generation and laser photolysis with a needle-based electrospray desorption mass spectrometry. With this strategy, individual droplets are irradiated with a single laser pulse and mass spectra are acquired from single droplets. Within seconds, photoproducts in the liquid droplet are detected with no cross-contamination and rapid laser-dependent signals are revealed using a consecutive laser-on/laser-off strategy. Each droplet provides a new, unphotolyzed and “clean” chemical volume allowing rapid

acquisition of thousands of single droplet measurements in minutes. This technique allows for the rapid identification of photo-labile species in solution environments. Capabilities of the instrumentation are demonstrated here with the 266 nm laser photolysis of methanol droplets containing 4-iodoaniline and 3-(iodomethyl)-*N*,*N*,*N*-trimethylbenzenamine.

Experimental

The experiment comprises a piezoelectric on-demand microdroplet generator, a thin steel needle held at +2.0 kV and a commercial ion trap mass spectrometer (Thermo Scientific LTQ Velos Pro). Microdroplets (~50 μm diameter) are produced on demand by a commercial microdroplet generator (Microdrop Technologies GmbH, MD-K-130, 50 μm inner nozzle diameter) that is driven by an amplified (FLC Electronics A400) square-wave pulse (190 $V_{0\text{-}P,}$ 35 μs duration) from a signal generator (Hameg HM8150). Each voltage pulse causes a contraction of the piezoelectric crystal within the droplet generator that, in turn, compresses a glass capillary expelling a portion of liquid from the capillary orifice. The timing of droplet generation is controlled by a trigger signal supplied by the mass spectrometer indicating the beginning of a scan. This trigger is first sent to a digital delay generator (SRS DG645) that then relays this to (i) the droplet signal generator, (ii) a pulsed LED used for droplet visualisation, and, when required, (iii) the pulsed photolysis laser. Synchronizing in this way ensures that a mass spectrum can be obtained from a single droplet. Droplets are typically generated at a frequency of ~10 Hz, however this rate varies with MS scan/isolation settings but ultimately, the droplet generation rate is dictated by the mass spectrometer. Triggering the droplet generation from the mass spectrometer ensures that any temporal changes to the MS sequence (*i.e.* additional ion trap isolation or CID steps) do not affect the droplet arrival time relative to the ion trap injection.

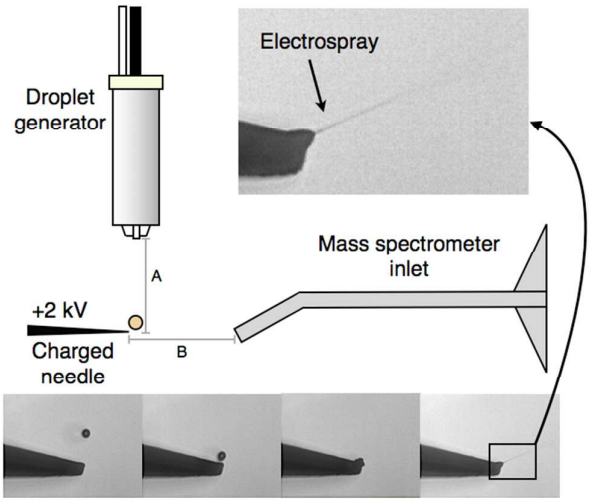

Figure 1 Schematic of the droplet electrospray arrangement. Distance A is ~2 mm and distance B ~3 mm. The inset images show the electrospray formation as the droplet encounters the charged needle.

The droplets free-fall ~2 mm at a velocity of ~1-2 ms^{-1} before impacting on a thin steel needle (Waters APGC corona discharge pin part # 700004809) held at ~+2.0 kV, supplied by a high voltage power supply (Canberra Instruments 3002D). At these voltages, methanol droplets are attracted towards the needle. The high electric field strength at the needle tip causes the droplet to distort and emit a spray (images shown in Figure 1). This spray is directed toward a transfer capillary attached at the inlet of the mass spectrometer. The needle voltage is maintained below that required to generate a corona discharge. Both the droplet generator and needle are mounted on independent 3-dimensional translation stages, allowing each to be precisely positioned relative to the transfer capillary to maximize the ion signal. The falling droplets and desorption process are monitored using a pulsed diode-based stroboscope arrangement perpendicular to the needle and transfer capillary axis. Varying the pulsed diode relative to droplet generation allows the process to be visualized and representative images are shown in the series of shadowgram stills seen in Figure 1. A schematic of this imaging

setup is shown in Figure S1. The droplet generator can be operated for many hours at 10 Hz without a misfire.

For laser photolysis experiments, single droplets are irradiated with one 266 nm laser pulse (~5 ns pulse width, ~30 mJ/cm^2) from a Nd:YAG laser (Continuum Minilite II) prior to interaction with the needle. The laser flashlamp is triggered by the digital delay generator allowing precise control of the droplet irradiation event, typically *ca.* 1 ms after the droplet generator is triggered. The diameter of the laser beam spot is approximately 3.5 mm upon reaching the droplet, which is large relative to the fall distance of the droplet. This allows the delay between droplet production and irradiation to vary without needing to adjust the laser beam position. The droplet generator tip is shielded to prevent irradiation by the laser and the laser beam path is adjusted to minimise irradiation of the needle. Droplet generation and the needle desorption are all performed under ambient laboratory conditions in air.

Results and Discussion

Using the experimental arrangement depicted in Figure 1, single droplet mass spectra are obtainable. Figure 2A shows a mass spectrum of one microdroplet containing 100 μM 4-iodoaniline in acidified (1% formic acid) methanol. The droplets have a diameter of ~50 μm corresponding to a volume of 65 pL. The number of analyte molecules present within each single microdroplet is therefore 6.5×10^{-15} mol or 3.9×10^{9} molecules. It is worthy to note there is significant scope for further dilution and smaller droplets, as there are at least four orders of magnitude of dynamic range on the ion count measurement. Control of distances A and B (see Figure 1) is vital to make adjustments for maximum ion signal.

Consecutive single microdroplet mass spectra are acquirable for extended time periods. To demonstrate the droplet-to-droplet reproducibility, the total ion counts from single droplet

mass spectra are followed over successive acquisitions. Figure 2B shows the ion count from 15 successive single droplet mass spectra, acquired over five seconds, with the MS ion trap scan cycle rate set at three times the droplet generation rate for the same conditions yielding the mass spectrum in Figure 2A. So with this timing scheme a droplet arrives at the needle every third MS injection cycle and therefore the single droplet mass spectra are distinguishable from MS cycles that do not correspond to the arrival of a droplet. The zero counts in between droplet spectra provide strong evidence that there is no significant cross contamination between droplet spectra and each spectrum comprises ions from the one droplet. Figure 2C displays the total ion signal chromatogram tracked over 1000 consecutive droplets under identical experimental conditions as Figure 2B. The average ion signal is 2.1 × 10^7 counts/s with a 2σ of 3.8 × 10^6 counts/s showing that the reproducibility is within 20% and this arrangement provides a stable platform for studying single droplet photochemical processes.

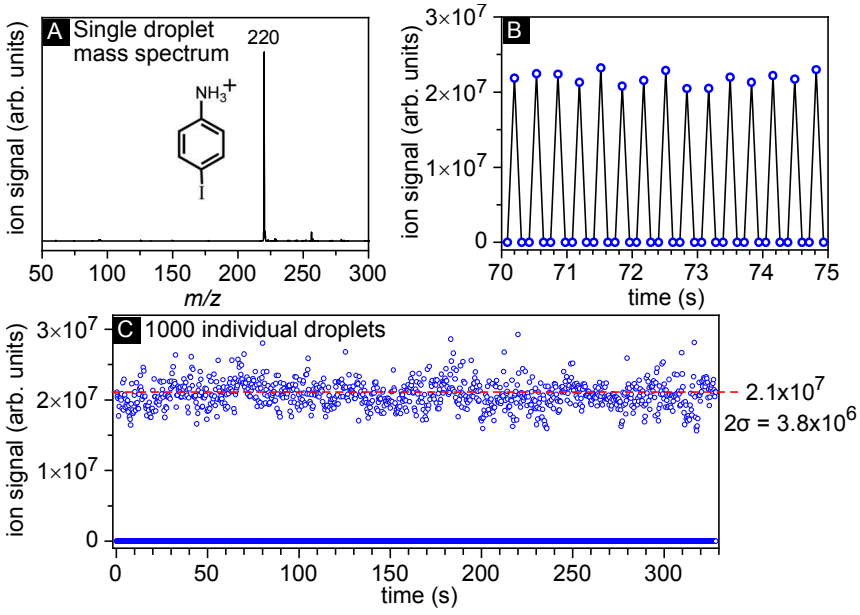

Figure 2 (A) Single droplet mass spectrum containing 100 μM 4-iodoaniline in acidified (1% formic acid) methanol, (B) time domain segment of 15 consecutive droplets where the mass

spectrometry acquisition time is set to three-times the droplet generation rate and (C) same experimental condition extended for 1000 consecutive droplets.

A single droplet mass spectrum acquired by the needle-based desorption technique can be compared to a mass spectrum acquired under conventional ESI conditions, for the same sample solution, on the same mass spectrometer (included as Figure S2 in the supporting information) and there is essentially no difference between the two methods for this solution and analyte.

The droplet desorption process occurs over a rather long period. Measurements show ions are detected over the droplet desorption event lasting ~20 ms (Figure S3 in the supporting information) which is less than the period of the triggering cycle which is on the order of hundreds of ms. Presumably, this desorption duration will depend on the droplet volume, the potential applied to the needle, the droplet velocity and the nature of the solvent, but we have not undertaken any study of these variables here. Using this technique we have also successfully employed water and acetonitrile as the droplet solvent (each acidified with 1% formic acid) for this desorption mass spectrometry technique. We suspect that solvent systems amenable to conventional electrospray ionization will also be suited to this droplet desorption technique. However, importantly, the technique also requires successful production of stable droplet trains, and for piezo-based droplet-on-demand methods, this depends on the liquid physical properties including viscosity, density and surface tension, as described in more detail in Reference [28].

To explore the signal response with changing concentration using this technique, a range of 3-chloroaniline standards (10 μM to 100 μM), referenced to an internal standard (aniline, 100

μM), were measured and a good fit to a linear trend is found (data shown in Supporting Information Figure S4). It reveals that for 3-chloroaniline, under these conditions and solvent, 10 μM is about the lower limit for direct detection.

To follow photochemistry in single droplets, a 266 nm laser pulse is timed to irradiate the droplet prior to it impacting the needle. Single droplet mass spectra are acquired with the laser alternating on and off, allowing the photoproducts to clearly be distinguished from background ions already in the solution. A comparison between the mass spectra for irradiated and non-irradiated droplets containing 100 μM 4-iodoaniline in methanol (1% formic acid), the same chemical system shown in Figure 2, is shown in Figure 3. Figure 3A is with the laser off and Figure 3B with the laser on. As is clear from Figure 3B, a new *m/z* signal appears at *m/z* 94 in addition to small peaks in the *m/z* 108-110 range. The laser-induced signal is more clearly highlighted in Figure 3C where the laser off spectrum is subtracted from laser on (after normalizing each spectrum to the total ion count), and laser dependent signals appear at *m/z* 94, 108 and 110. The peak at *m/z* 94 can be rationalised by the photolysis of protonated 4-iodoaniline that loses the I atom,[22] leaving the ammonium phenyl radical (*m/z* 93) and this reactive species abstracts a H atom from the methanol solvent to form protonated aniline (*m/z* 94) (Scheme 1). This is consistent with the reactions of charge-tagged phenyl radicals by Kenttamaa and coworkers.[23] The ions responsible for *m/z* 108 and 110 are plausibly the addition of a methyl and hydroxyl group to the radical site, respectively. At the laser fluences utilised, no significant ions are detected when the needle voltage is held at 0 V, suggesting laser desorption/ionisation is not affecting these experiments.

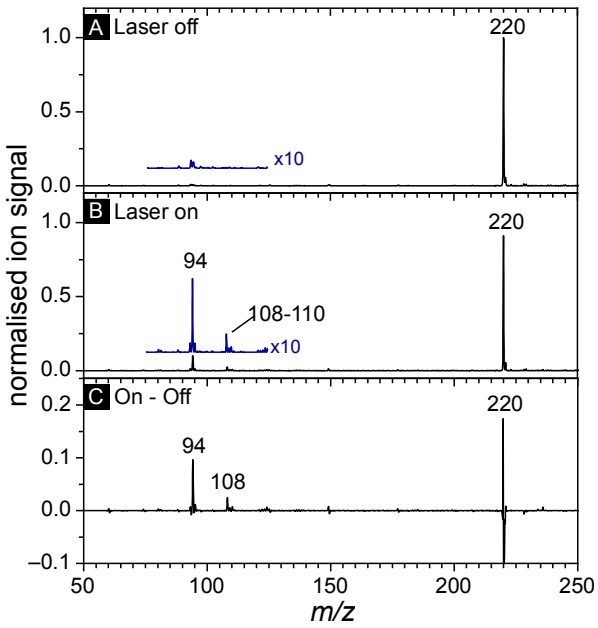

Figure 3 Single microdroplet mass spectra acquired without UV (λ = 266 nm) laser irradiation (A) and with UV laser irradiation (B) prior to needle impact. Each spectrum is the average of 400 single microdroplet mass spectra. (C) Difference spectrum of laser on (B) and laser off (A) spectra.

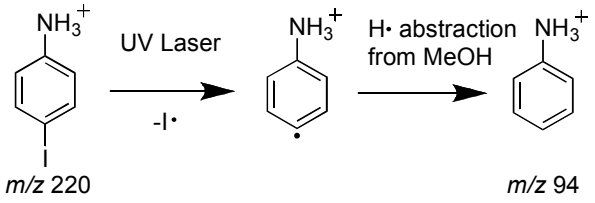

Scheme 1

Tracking the photolysis yield of the main photoproduct at *m/z* 94 is possible by triggering the laser at half the rate of the droplet generator, such that every second droplet is irradiated. A large data set is rapidly accumulated revealing the laser dependent production of *m/z* 94. An example of this is presented in Figure 4. The background *m/z* 94 ion signal level is 1.1×10^5 with a statistical 2σ of 1.2×10^4 increasing to 5.2×10^5 ($2\sigma = 1.3 \times 10^5$) with laser irradiation

(266 nm, 30 mJ/cm^2). The sizable standard deviation of the photoproduct ion signal is probably due to fluctuations in pulse intensity from the photolysis laser – owing to the 266 nm laser radiation being generated from two successive non-linear optical processes. The product yield of *m/z* 94 has also been measured as a function of laser power and, within this fluence regime (~30 mJ/cm^2), displays a linear dependence that is consistent with a single-photon mediated process (see Figure S5 of the Supporting Information).

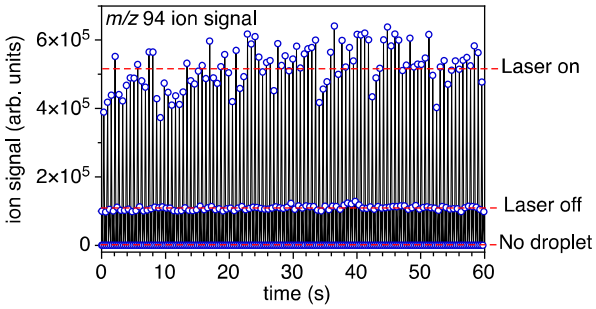

Figure 4 Ion counts of single droplet mass spectra of 200 consecutive droplets, where m/z 94 has been isolated in the ion trap. Mass spectrometer acquisition rate is ×2 faster than that of droplet production and ×4 that of laser pulse rate.

In principle, these photodissocation data could be used to quantify the photolysis yield of the *m/z* 94 photoproduct at 266 nm in picolitre-volumes of solution. With known photon fluence, absorption cross-section and photoproduct peak areas known relative to the parent, a value for the photolysis should be obtainable. The laser fluence can be measured and corrected for a 50 μm diameter spherical volume as described by Mayer *et al.*[24] The absorption cross section of the spherical droplets may be determined by applying the Beer-Lambert law corrected for a spherical particle using a method such as that described by Kim *et al.*[25] Peak areas relative to the parent molecule peak determined via mass spectrometry need to be corrected for detection efficiencies using standards (this is explored further in supporting information, Figure S2).

Single droplet processes such as whispering gallery modes[26] and surface enhancement effects[27] may have significant influence on these yields, although for aerosol applications these 50 μm droplets are rather large. Nevertheless, the study of single aerosol droplet photochemistry is an application of this technique, and can be easily extended to incorporate tunable photon sources. Smaller diameter droplets can be generated using these methods by applying more complex waveforms to the piezoelectric droplet generator.[28] Some other soft ionization methods have recently emerged to directly probe aerosol particles including direct analysis in real time (DART) mass spectrometry.[29, 30]

Benzyl

A benzyl type radical precursor, 3-(iodomethyl)-*N*,*N*,*N*-trimethylbenzenamine (structure shown in Figure 5 inset), was also investigated using the same single droplet photolysis strategy. As a native cation, a lower concentration solution of 10 μM was required to yield similar ion signal intensity. The expected radical, formed through C—I bond homolysis is π-type resonance-stabilized and thus different reactivity may be expected to the phenyl radical system above. The difference between the mass spectra of 400 irradiated and 400 unirradiated acidified (1% formic acid) methanolic droplets (containing 3-(iodomethyl)-*N*,*N*,*N*-trimethylbenzenamine), is presented in Figure 5, several laser dependent ion signals are detected. Laser dependent signals at *m/z* 60 (**A**), 136 (**B**), 150 (**C**), 164 (**D**), 166 (**E**), 180 (**F**) and 262 (**G**) are evident, with proposed structures shown in Figure 6. Photoproduct **A** is assigned as the trimethyl ammonium formed from homolysis of the C-N bond and subsequent abstraction of H from the methanol solvent. **B** and **F** are assigned as products of laser homolysis of the C-I bond and subsequent addition of H atom and methoxy (CH_3O), respectively, from the methanol solvent. **D** and **E** are plausibly formed via reaction with dissolved O_2, consistent with previous studies of benzyl radicals in methanol.[31] **G** is proposed

to result from homolysis of the bond between the nitrogen and one of the methyl groups, followed by H abstraction from the methanol solvent. The photolysis of this system demonstrates the many photolysis pathways of this ion in solution at λ = 266 nm. Furthermore, these different photofragment ions then proceed to react with either the solvent or other species in solution (in this case, putative reactions with dissolved O_2), and because the droplet has only sustained one laser pulse, it can be confidently asserted that all photoproducts originate from the same precursor – rather than successive photochemistry. Future studies will need to investigate whether any of this chemistry is unique to the microdroplet environment and the significant surface area to volume ratio.

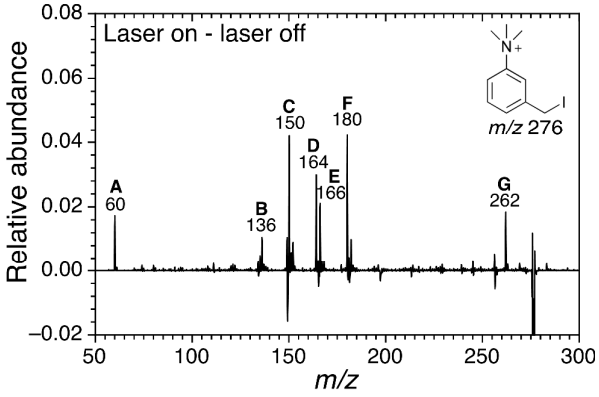

Figure 5 The difference mass spectrum from irradiated (laser on, average of 400 single droplet mass spectra) and unirradiated (laser off, average of 400 single droplet mass spectra) droplets containing 10 μM 3-(iodomethyl)-*N*,*N*,*N*-trimethylbenzenamine. Positive signal identifies laser dependent products.

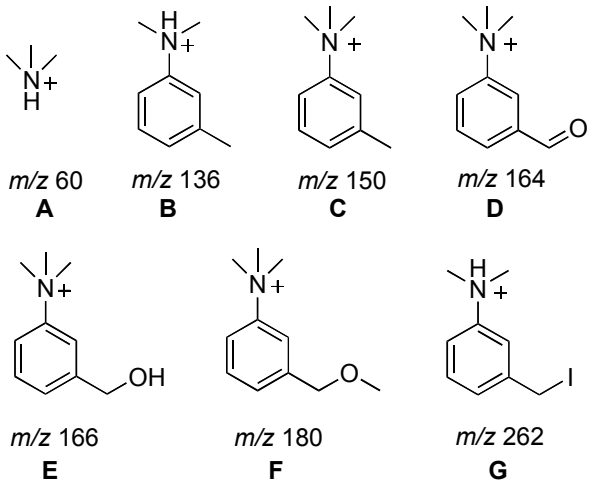

Figure 6 Proposed structures for the main products detected following photolysis of acidified (1% formic acid) methanolic 3-(iodomethyl)-*N*,*N*,*N*-trimethylbenzenamine droplets.

Conclusions

It is demonstrated that single droplet mass spectra are recordable, one droplet at a time, using a needle desorption electrospray technique and an on-demand microdroplet generator coupled to a commercial ion trap mass spectrometer. By incorporating a pulsed laser to selectively irradiate the single droplets, photochemical products are rapidly detected by comparing to unirradiated droplets from successive laser-on/laser-off experiments. In tens of seconds photoproducts can be detected and identified from only a few tens of droplets – corresponding to several hundred picolitres of sample. This reported strategy is suitable for the study of photoactive molecules where direct photodissociation is unwanted – *e.g.* in many photodynamic therapies – and can also be applied for the study of aerosol photochemistry and monitoring photosynthetic chemistry.

Supporting Information

Additional information in supplied as referred to in the main text. This material is available free of charge via the Internet at http://pubs.acs.org.

Acknowledgements

The authors gratefully acknowledge funding support from the Australian Research Council (DP1094135, DP120102922) and infrastructure support from the University of Wollongong. BLJP acknowledges funding support through the ARC DECRA program (DE120100467). Prof. Stephen Blanksby (University of Wollongong) is acknowledged for many helpful discussions, as is Mr James Bezzina for assistance in the early stages of this project.

References

1. Poschl, U. *Angew. Chem., Int. Ed.*, **2005**, *44,* 7520-7540.

2. Epstein, S. A.; Tapavicza, E.; Furche, F.; Nizkorodov, S. A. *Atmos. Chem. Phys.*, **2013**, *13,* 9461-9477.

3. Monge, M. E.; Rosenorn, T.; Favez, O.; Muller, M.; Adler, G.; Riziq, A. A.; Rudich, Y.; Herrmann, H.; George, C.; D'Anna, B. *Proc. Natl. Acad. Sci. U. S. A.*, **2012**, *109,* 6840-6844.

4. El Ghissassi, F.; Baan, R.; Straif, K.; Grosse, Y.; Secretan, B.; Bouvard, V.; Benbrahim-Tallaa, L.; Guha, N.; Freeman, C.; Galichet, L.; Cogliano, V. *The Lancet Oncology*, **2009**, *10,* 751-752.

5. Friedberg, E. C. *Nature*, **2003**, *421,* 436-440.

6. Goodsell, D. S. *The Oncologist*, **2001**, *6,* 298-299.

7. Huang, Z. *Technol. Cancer Res. Treat.*, **2005**, *4,* 283-293.

8. Dolmans, D. E. J. G. J.; Fukumura, D.; Jain, R. K. *Nat. Rev. Cancer*, **2003**, *3,* 380-387.

9. Cremer, R. J.; Perryman, P. W.; Richards, D. H. *The Lancet*, **1958**, *271,* 1094-1097.

10. Glauser, S. C.; Lombard, S. A.; Glauser, E. M.; Sisson, T. R. C. *Exp. Biol. Med.*, **1971**, *136,* 518-519.

11. Chen, J.; Keltner, L.; Christophersen, J.; Zheng, F.; Krouse, M.; Singhal, A.; Wang, S. *Cancer J.*, **2002**, *8,* 154-163.

12. Wilson, B. *Can. J. Gastroenterol.*, **2002**, *16,* 393 - 396.

13. Vrouenraets, M. B.; Visser, G. W. M.; Snow, G. B.; van Dongen, G. *Anticancer Res.*, **2003**, *23,* 505-522.

14. Grimm, R. L.; Beauchamp, J. L. *J. Phys. Chem. B*, **2003**, *107,* 14161-14163.

15. Grimm, R. L.; Beauchamp, J. L. *J. Phys. Chem. B*, **2005**, *109,* 8244-8250.

16. Jorabchi, K.; Westphall, M. S.; Smith, L. M. *J. Am. Soc. Mass Spectrom.*, **2008**, *19,* 833-840.

17. Westphall, M. S.; Jorabchi, K.; Smith, L. M. *Anal. Chem.*, **2008**, *80,* 5847-5853.

18. Hager, D. B.; Dovichi, N. J. *Anal. Chem.*, **1994**, *66,* 1593-1594.

19. Hager, D. B.; Dovichi, N. J.; Klassen, J.; Kebarle, P. *Anal. Chem.*, **1994**, *66,* 3944-3949.

20. Laskin, J.; Laskin, A.; Nizkorodov, S. A. *Int. Rev. Phys. Chem.*, **2013**, 1-43.

21. Kim, H. I.; Kim, H.; Shin, Y. S.; Beegle, L. W.; Goddard, W. A.; Heath, J. R.; Kanik, I.; Beauchamp, J. L. *J. Phys. Chem. B*, **2010**, *114,* 9496-9503.

22. Hansen, C. S.; Kirk, B. B.; Blanksby, S. J.; O'Hair, R. A. J.; Trevitt, A. J. *J. Am. Soc. Mass Spectrom.*, **2013**, *24,* 932-940.

23. Thoen, K. K.; Smith, R. L.; Nousiainen, J. J.; Nelson, E. D.; Kenttämaa, H. I. *J. Am. Chem. Soc.*, **1996**, *118,* 8669-8676.

24. Mayer, B.; Madronich, S. *Atmos. Chem. Phys.*, **2004**, *4,* 2241-2250.

25. Kim, H. B.; Yoshida, S.; Kitamura, N. *Anal. Chem.*, **1998**, *70,* 51-57.

26. Symes, R.; Sayer, R. M.; Reid, J. P. *Phys. Chem. Chem. Phys.*, **2004**, *6,* 474-487.

27. Nissenson, P.; Knox, C. J. H.; Finlayson-Pitts, B. J.; Phillips, L. F.; Dabdub, D. *Phys. Chem. Chem. Phys.*, **2006**, *8,* 4700-4710.

28. Chen, A. U.; Basaran, O. A. *Phys. Fluids*, **2002**, *14,* L1-L4.

29. Chan, M. N.; Nah, T.; Wilson, K. R. *Analyst*, **2013**, *138,* 3749-3757.

30. Nah, T.; Chan, M.; Leone, S. R.; Wilson, K. R. *Anal. Chem.*, **2013**.

31. Meiggs, T. O.; Grossweiner, L. I.; Miller, S. I. *J. Am. Chem. Soc.*, **1972**, *94,* 7981-7986.

For TOC only: